**AAV-mediated ERdj5 overexpression protects against P23H rhodopsin toxicity**

Monica Aguilà[1], James Bellingham[1], Dimitra Athanasiou[1], Dalila Bevilacqua[1], Yanai Duran[1], Ryea Maswood[1], David A Parfitt[1], Takao Iwawaki[2], Giannis Spyrou[3], Alexander J Smith[1], Robin R Ali[1] and Michael E Cheetham[1*]

[1]UCL Institute of Ophthalmology, 11-43 Bath Street, London EC1V 9EL, UK

[2]Division of Cell Medicine, Department of Life Science, Medical Research Institute, Kanazawa Medical University, Uchinada, Japan.

[3]Department of Clinical and Experimental Medicine, Linköping University, Linköping, Sweden

*To whom correspondence should be addressed

Professor Mike Cheetham, UCL Institute of Ophthalmology, 11-43 Bath Street, London EC1V 9EL UK.

Tel +44 (0)20 7608 6944 Fax +44(0)20 7608 6892

email michael.cheetham@ucl.ac.uk

**Abstract**

Rhodopsin misfolding caused by the P23H mutation is a major cause of autosomal dominant retinitis pigmentosa (adRP), to date there are no effective treatments for adRP. The BiP co-chaperone and reductase ERdj5 (DNAJC10) is part of the ER quality control machinery and previous studies have shown that overexpression of ERdj5 *in vitro* enhanced the degradation of P23H rhodopsin; whereas knockdown of ERdj5 increased P23H rhodopsin ER retention and aggregation. Here, we investigated the role of ERdj5 in photoreceptor homeostasis *in vivo* by using an *Erdj5* knock-out mouse crossed with the P23H knock-in mouse, and by adeno associated viral (AAV) vector-mediated gene augmentation of ERdj5 in P23H-3 rats. Electroretinogram (ERG) and optical coherence tomography (OCT) of *Erdj5*$^{-/-}$ and *P23H*$^{+/-}$:*Erdj5*$^{-/-}$ mice showed no effect of ERdj5 ablation on retinal function or photoreceptor survival. Rhodopsin levels and localisation were similar to those of control animals at a range of time points. By contrast, when AAV2/8-ERdj5-HA was subretinally injected into P23H-3 rats, analysis of the full field ERG suggested that overexpression of ERdj5 reduced visual function loss 10 weeks post-injection. This correlated with a significant preservation of photoreceptor cells at 4 and 10 weeks post-injection. Assessment of the outer nuclear layer (ONL) morphology showed preserved ONL thickness and reduced rhodopsin retention in the ONL in the injected superior retina. Overall, these data suggest that manipulation of the ER quality control and ERAD factors to promote mutant protein degradation could be beneficial for the treatment of adRP caused by mutant rhodopsin.

2

**Introduction**

Retinitis Pigmentosa (RP) is a group of retinal degenerative diseases that are characterized primarily by the loss of rod photoreceptor cells (1). RP is the most common cause of genetic blindness and affects approximately 1 in 3000 individuals in the United States (2). Individuals with RP experience night blindness, a progressive loss of peripheral visual fields and eventually loss of central vision as cone photoreceptor viability is compromised by rod cell death (3). Mutations in rhodopsin are a major cause of autosomal dominant RP, with over 200 mutations identified (4). In particular, the proline to histidine change at residue 23 (P23H) is a commonly studied mutation; indeed, it is the most common rhodopsin mutation found in North America (5). Rhodopsin mutations can be classified according to their molecular and cellular properties and P23H belongs in the class II group of mutations, characterized by misfolding and intracellular inclusion formation (4, 6). The P23 residue resides in the intradiscal domain of rhodopsin and its substitution causes misfolding of the protein, reduces the 11-*cis*-retinal binding capability of rhodopsin and thus results in loss of function (7).

Misfolding of rhodopsin results in retention of the protein in the ER and subsequent degradation via the ubiquitin-proteasome system via ER-associated degradation (ERAD) (4). The folding and stability of rhodopsin are dependent on the formation of a disulfide bond between cysteine residues at positions 110 and 187 (C110 and C187) (8). Misfolded rod opsin can form a non-native disulfide bond between C185 and C187 (or C110 and C185 etc.), which traps rhodopsin in a misfolded state and causes loss of retinal binding (9).

3

Within the cell, networks of systems are responsible for maintaining correct protein function and homeostasis, known as proteostasis. Proteostasis mechanisms include systems for refolding, sequestering and degrading misfolded proteins, such as molecular chaperones, the unfolded protein response (UPR) and ERAD (10). Molecular chaperone proteins are important cellular factors for dealing with misfolded proteins. In particular, the ER resident HSP70 family member BiP (HSPA5) is involved in regulating the UPR and assisting the folding of ER synthesized proteins (11). The UPR helps to clear misfolded proteins by activating a transcriptional program that upregulates expression of molecular chaperones, degradation pathways and apoptosis mechanisms, but also reduces the transcriptional load on the cell (12). Furthermore, BiP is involved in the normal biogenesis of rhodopsin, as well as the quality control of misfolded forms of rhodopsin (13), and BiP overexpression is protective in a P23H transgenic rat model (14). BiP function is regulated by ER-resident co-chaperones from the DNAJ family, of which there are several, including ERdj5 (15).

ERdj5 (also known as J-containing PDI-like protein (JPDI), or DNAJC10) is a multidomain protein containing a J-domain that interacts with BiP and six thioredoxin-like (TRX) domains. Of these TRX domains, four are active and contain CXXC motifs (16-18). ERdj5 has a role in ERAD for both glycosylated and non-glycosylated misfolded proteins, and can act via its TRX domains as reductase for incorrect disulfide bonds in misfolded proteins, such as the one formed in misfolded P23H rhodopsin (19).

Another important component in rhodopsin proteostasis is the ER degradation-

4

enhancing alpha-mannosidase-like 1 (EDEM1). EDEM1 enhances ERAD of terminally misfolded glycoproteins (20, 21). We have previously shown that EDEM1 has dual activity towards mutant rhodopsin *in vitro* as it enhanced the degradation of P23H rod opsin and also promoted its correct folding (22). Moreover, EDEM1 is expressed in photoreceptors and can be co-immunoprecipitated with WT rhodopsin from the ER (22). EDEM1 has also been shown to bind to cone opsin in 11-*cis*-retinal deficiency (23).

BiP and EDEM1 activity is coupled by ERdj5 to promote ER quality control and ERAD (18, 24). The degradation of mutant rhodopsin *in vitro* by ERdj5 requires the combined activity of the J domain to recruit BiP, and the thioreductase function (19), suggesting that ERdj5 could act as an important component of the ER quality control and degradation machinery in photoreceptors.

In this study, we investigated the effect of ERdj5 *in vivo* using an *Erdj5* knock-out mouse (25). These animals are viable and healthy, but show ER stress at sites of heavy protein secretion (e.g. salivary gland). Therefore, we also tested if *Erdj5* deletion might cause photoreceptor defects that would be more pronounced in the presence of proteotoxic stress from mutant rhodopsin. Furthermore, we tested whether increasing the levels of ERdj5 through gene augmentation could protect photoreceptors from P23H rhodopsin mediated cell death.

**Results**

**ERdj5 knockout mice do not show retinal degeneration**

To examine the role of ERdj5 in photoreceptors we investigated the retina of *Erdj5*-knockout mice. ERdj5 was detectable by Western blot in control, wild-type (WT)

5

retina, but was absent in *Erdj5* knock-out (*Erdj5*<sup>-/-</sup>) confirming that ERdj5 is normally present in retina and that the knock-out lacks ERdj5 expression (Figure 1A). Rhodopsin electrophoretic mobility and levels assessed by Western blot were indistinguishable between *Erdj5*<sup>-/-</sup> and WT animals (Figure 1A). Photoreceptor function was assessed by a full field scotopic electroretinogram (ERG) in dark-adapted mice at P70 and P200. Increasing light intensity correlates with a greater response of photoreceptor hyperpolarisation (a-wave), followed by the propagation of the signal through the retina with subsequent depolarisation (b-wave). *Erdj5*<sup>-/-</sup> mice showed unaffected ERG responses, as both a-wave and b-wave response amplitudes were similar to those of the WT control mice at both time points (Figure 1B and 1C). These data suggest that lack of ERdj5 does not impair visual function. Optical coherence tomography (OCT) was used to measure the thickness of the outer nuclear layer (ONL), as a marker of photoreceptor survival. The measurement of the ONL across the whole retina showed *Erdj5*<sup>-/-</sup> mice had the same ONL thickness as WT mice suggesting the retina was healthy (Figure 1D). There was also no difference in their ONL thickness in the superior or inferior retina (Figure 1E). To confirm this observation, the retina of *Erdj5*<sup>-/-</sup> and WT mice were analyzed by histology (Figure 1F). The ONL thickness and rhodopsin localization of *Erdj5*<sup>-/-</sup> mice were indistinguishable from the WT. Overall, no adverse effects of *Erdj5* knockout were observed in the retina.

**ERdj5 ablation in rhodopsin P23H mice does not affect retinal degeneration**

ERdj5 facilitates degradation of misfolded proteins via ERAD (26); therefore, ablation of *Erdj5* could exacerbate retinal degeneration in P23H rhodopsin mouse models. To determine the effect of lack of ERdj5, we crossed P23H knock-in (KI; *P23H*<sup>+/-</sup>) (27) mice with *Erdj5* knock-out mice to produce *P23H*<sup>+/-</sup>:*Erdj5*<sup>-/-</sup> and

6

compared them to littermate *P23H^{+/-}:Erdj5^{+/+}* animals. The *P23H^{+/-}* mice have a moderate retinal degeneration phenotype with rod photoreceptor cell almost complete at 170 days of age (27). Therefore, we assessed visual function of the *P23H^{+/-}:Erdj5^{-/-}* animals at P70, a stage where the *P23H^{+/-}* animals show clear rod cell dysfunction and death, but there are still photoreceptors remaining, enabling changes in the rate of disease in either direction to be observed. Scotopic ERG responses were similar in the presence and absence of ERdj5 (Figure 2A). ONL thickness measurements assessed by OCT also revealed no difference, either in the total retina (Figure 2B), or in the superior or inferior hemispheres (Figure 2C). Immunohistochemistry of the *P23H^{+/-}:Erdj5^{-/-}* retina showed no difference in retinal structure or rhodopsin localization to the P23H controls (Figure 2D). The levels of rhodopsin expression assessed by Western blot remained unchanged (Figure 2E). These results suggest that loss of ERdj5 does not affect the photoreceptor response to misfolded rhodopsin.

**Subretinal delivery of AAV2/8-ERdj5 reduces the loss of P23H-3 rhodopsin photoreceptors**

Previous *in vitro* data showed that overexpression of ERdj5 could promote P23H rhodopsin degradation, reduce aggregation and inclusion formation (19). To investigate the effect of ERdj5 overexpression on P23H *in vivo*, we used adeno-associated viral (AAV) mediated transduction of photoreceptors in the P23H-3 rat model. The rat model was chosen because the larger size of the rat eye facilitated sub-retinal injection, and this model has a well characterized rate of degeneration similar to the P23H KI mouse model. P23H-3 rhodopsin rats received subretinal injections of either an AAV2/8 vector carrying ERdj5 with an HA tag (AAV2/8-ERdj5-HA) virus or PBS to the superior retina at P15. Following injection, we analyzed animals over three months by ERG and OCT and then euthanized them for histological and

7

immunochemical analysis.

Overexpression of ERdj5 in P23H-3 rats led to no difference in the ERG responses between the PBS and the ERdj5 injected eyes 4 weeks post-injection (Figure 3A). 10 weeks after injection, slightly better responses were observed in the eyes that had received ERdj5, but these did not reach statistical significance (Figure 3B). OCT measurement 4 weeks post injection for the AAV2/8-ERdj5-HA injected eyes showed significant preservation of ONL thickness across the retina (Figure 3D and 3E). By 10 weeks post-injection, there was not a significant change in ONL thickness in the treated eyes when measured across the whole retina. However, in the superior hemisphere of the retina, where the injection was performed, we observed a significant preservation of ONL thickness in the AAV2/8-ERdj5-HA injected eyes compared to the PBS injected retinae at both time points (Figure 3F and 3G).

A strong HA signal was detected in the inner segment (IS), where ERdj5 is expected to localize (Figure 3H). The signal was restricted to the superior hemisphere of the retina where the subretinal injection was performed and was not detected in the inferior hemisphere. Histological analyses also confirmed that the AAV2/8-ERdj5-HA transduced retinae were thicker in the superior part, as they showed an extra photoreceptor nuclei layer compared to the PBS injected retinae (Figure 3H). These data suggest that Erdj5 overexpression is protective in P23H-3 rats.

**ERdj5 overexpression promotes rhodopsin degradation in P23H rats**

Immunohistological analysis of the treated retinae at 4 and 10 weeks post injection revealed differences in rhodopsin localization between the superior and inferior retina (Figure 4A). Quantification of fluorescence intensity in the ONL revealed a significant decrease in mislocalized rhodopsin in the superior retina, where there was a strong HA signal, at both time points compared to the inferior retina (Figure 4B).

8

This was in contrast to the PBS injected retina, where the superior and inferior retina were similar in intensity (Figure 4C). To investigate whether ERdj5 could form a complex with rhodopsin, retinal lysates were co-immunoprecipitated with an antibody against the HA epitope and blotted with an antibody to rhodopsin. Rhodopsin was enriched when co-immunoprecipitated with ERdj5-HA in the AAV2/8-ERdj5-HA injected eyes, whereas background levels of rhodopsin were detected in PBS-injected eyes with anti-HA, or with a control IgG immunopurification in AAV2/8-ERdj5-HA treated retina (Figure 4D). These data suggest that overexpressed ERdj5 can form a complex with rhodopsin *in vivo*. Retinal lysates of PBS and AAV2/8-ERdj5-HA injected eyes were blotted with 1D4 (Figure 4E) and rhodopsin levels were quantified (Figure 4F). ERdj5 injected retinae showed less rhodopsin compared to the PBS injected retinas; however, this difference did not reach statistical significance. Collectively, these data suggest that ERdj5 overexpression can promote mutant rhodopsin clearance from the ER and enhance photoreceptor survival.

**Discussion**

The results in this study suggest that ERdj5 is not essential for rhodopsin biogenesis or function *in vivo*. Nor did loss of ERdj5 have an effect on P23H rhodopsin expression, localization or pathogenicity. This is in contrast to what was observed *in vitro*, where knock-down of ERdj5 affected the expression of both WT and P23H rod opsin in SK-N-SH neuroblastoma cells (19). The cause of this difference is not clear, but most likely relates to the heterologous overexpression system not fully reflecting the situation in photoreceptors. For example, heterologous rod opsin overexpression could affect ER protein loading, and there was no 11-*cis*-retinal present in this system, and retinoids are known to affect P23H folding (4). Similarly, the repertoire of ER

9

chaperones in cultured cells might not accurately reflect the situation in photoreceptors. It has been suggested that different ER chaperones, such as PDI family proteins, other chaperones and DnaJ proteins, and ERdj5 have a redundant function in the ER protein quality control (28). This might explain why the lack of ERdj5 does not affect retinal degeneration, as other ER components are potentially compensating for its absence. Similarly, the photoreceptor ER quality control and ERAD machinery might be adapted to have less need for ERdj5.

By contrast, salivary gland function appears to require ERdj5, as ERdj5 ablation leads to a Sjögren's Syndrome-like phenotype in mice with induction of the UPR and the infiltration of immune cells, similar to that observed in patients (29). These data confirm the initial studies that the loss of ERdj5 principally affects the salivary gland (25), and is less critical in other tissues, where the requirement for coupling co-chaperone, reductase and ERAD for misfolded proteins is probably met by other factors.

Gene therapy approaches for dominant retinal disease, such as P23H rhodopsin RP, are more challenging than classical gene replacement/augmentation. Although gene augmentation with WT rod opsin has shown some benefit in P23H transgenic mice (30), supporting a dominant negative contribution to the pathogenesis, the majority of approaches have focused on either promoting photoreceptor survival in a gene independent way, or targeting the mutant allele. For example, allele specific knockdown of the mutant transcript through ribozymes or antisense oligonucleotides (31, 32), non-specific knockdown of both alleles with gene replacement (33, 34), or CRISPR based gene editing (35, 36). Here, we show that viral-mediated overexpression of ERdj5 can improve photoreceptor viability in P23H rats. These results suggest that manipulation of ER quality control and ERAD factors could

10

potentially benefit misfolding mutations in rhodopsin RP.

ERdj5 is a co-chaperone for BiP, which has also been suggested to play an important role in rhodopsin proteostasis (13, 14). Indeed, overexpression of BiP also protects against P23H rhodopsin mediated photoreceptor cell death (14). Studies of the P23H KI mouse have shown that over 90% of the mutant protein is degraded (27, 37). Nevertheless, the P23H that escapes ER quality control and reaches the outer segment has detrimental effects on outer segment structure (27, 38), and pharmacologically enhanced traffic of P23H rhodopsin to the outer segment accelerated retinal degeneration (39). Furthermore, expression of P23H rhodopsin has been suggested to induce ER stress (4). Whether this contributes to cell death is not certain, but the enhanced load on the photoreceptor proteostasis machinery and potential inhibition of protein degradation, have also been implicated in photoreceptor cell death (4). Therefore, enhanced photoreceptor proteostasis and/or degradation of the mutant protein could promote photoreceptor survival.

Overexpression of ERdj5 led to reduced retention of rhodopsin in the ONL of P23H rat retina, this was only observed in the transduced areas of the retina and correlated with improved photoreceptor viability. There was a small reduction in the total amount of rhodopsin and a mild improvement in ERG, neither of which reached statistical significance. Full-field ERGs measure the response from the entire retina. Parallel injections with a AAV2/8:GFP indicated that photoreceptor transduction was also limited to the superior retina and approximately 50% of the photoreceptors in this region were transduced (data not shown), suggesting only 25% of total photoreceptors would be transduced, which might reduce the potential for an increase to a full field ERG and limit any effect on total rhodopsin protein. The reduction in ONL staining for rhodopsin and total rhodopsin protein suggests improved clearance of rhodopsin

11

from the ER. The ability of the transduced ERdj5-HA to bind rhodopsin suggests this effect could be directly mediated by ERdj5 facilitating ERAD of the mutant protein.

It is important that any approach to enhance mutant rhodopsin degradation does not target the WT protein, as rod photoreceptors need sufficient rhodopsin to maintain viability (40). Unfortunately, we cannot discriminate between the WT and P23H protein in our assays as they only differ at a single residue, so we cannot determine if ERdj5 is specifically enhancing the clearance of the mutant protein or acting on WT rhodopsin, or even on other proteins. Nevertheless, *in vitro* studies showed that ERdj5 binds preferentially to P23H rod opsin (19), and in studies of other retinal disease genes, such as the R345W mutation in fibulin 3, ERdj5 also preferentially binds to the mutant protein (41). The correlation of the reduction in rhodopsin ER retention and improved cell viability support the notion that the mutant protein clearance is enhanced and other photoreceptor proteins, including WT rhodopsin, are not adversely affected.

These data support the hypothesis that enhancing the degradation of mutant rhodopsin through the delivery of important chaperones or ERAD factors could enhance photoreceptor survival in adRP. Previous studies of BiP gene delivery and proteasomal upregulation also support this concept (14, 42). This approach could be used to complement other approaches that promote photoreceptor survival or target the mutant allele, such as allele specific knock-down, to further lower the threshold of mutant protein expression and block toxic gain of function effects.

**Acknowledgements**

## Materials and Methods

### Animals

All animal procedures were conducted according to the Home Office (UK) regulations, under the Animals (Scientific Procedures) Act of 1986, and with the approval of the local UCL Institute of Ophthalmology, London, UK ethics committee. The P23H-3 line rats were kindly provided by Professor Matt LaVail, (University of California San Francisco, USA, http://ophthalmology.ucsf.edu/wp-content/uploads/LaVail-RD-Rat-Model-Resource-063011.pdf) and crossed with wild-type Sprague Dawley (SD) rats to generate heterozygous P23H-3 rats. SD rats were purchased from Harlan (Blackthorn, UK). *P23H* KI mice were generated as previously described (27). *Erdj5* knock-out mice (*Erdj5*$^{-/-}$) were generated as previously described (25). All animals were housed under a 12 h light (20–100 lux): 12 h dark (<10 lux) cycle, with food and water available *ad libitum*. Both sexes were used evenly for experiments.

### Plasmid Construct, Production of AAV and Intraocular Administration

13

In order to preserve the Inverted Terminal Repeat (ITR) sites of the pD10-CMV backbone yet create a more flexible multiple cloning site, the eGFP sequence was deleted from pEGFP-N1 vector (Clontech) by site directed mutagenesis (NEB Q5 Site Directed Mutatgenesis Kit) using the following primers, delGFP_F: 5'-AAGCGGCCGCGACTCTAG-3' and delGFP_R: 5'-CGACCGGTGGATCCCGGG-3', to produce pCMV-delGFP. Subsequently, the multiple cloning site from pCMV-delGFP was excised with *NcoI* and *NotI* and cloned into the *NcoI* and *NotI* sites of pD10-CMV-GFP to create pD10-CMV-delGFP. The mouse ERdj5:HA:KDEL was excised from its pcDNA3.1(+) backbone (19, 43) with *NheI* and *ApaI* and cloned into *NheI* and *ApaI* sites of pD10-CMV-delGFP to create pD10-CMV-ERdj5-HA-KDEL. NEB Stable Competent *E. Coli* cells were used throughout to protect the integrity of the ITRs.

Recombinant AAV2/8 serotype particles were produced through a previously described triple transient transfection method HEK293T cells (44). AAV2/8 serotype particles were bound to an AVB Sepharose column (GE Healthcare) and eluted with 50 mM glycine pH 2.7 into 1 M Tris pH 8.8. Vector was washed in PBS and concentrated to a volume of 100–150 μL using Vivaspin 4 (10 kDa) concentrators. Viral genome titre was determined by quantitative real-time PCR using a probe-based assay binding the SV40 poly-adenylation signal.

Viral vector administration was performed under general anaesthesia using an operating microscope (CarlZeiss) and a 34G needle (Hamilton). A total volume of 4uL AAV2/8-Erdj5-HA was injected into P23H-3 rats at P15. Contralateral eyes were injected with PBS.

14

**Electroretinography (ERG)**

Animals were dark-adapted overnight in a ventilated light-tight box and anaesthetised with either ketamine/xylazine at 0.2 ml/100 g (rats) or with ketamine/domitor at 0.08 ml/10 g (mice) administered via an IP injection. Full-field scotopic ERG was carried out using the Diagnosys system and Espion software (Diagnosys, Lowell, MA) under red-light conditions, as previously described (39). Briefly, simultaneous bilateral recordings were taken using scotopic ERG protocols. Flash stimuli (10 ms to 1 ms duration, repetition rate 0.2 Hz) were presented via an LED stimulator (log intensity -5 to + 1) under scotopic conditions. ERG responses were collected with the Espion software for analysis. Statistical analysis was performed using 2 tailed Student's $t$ test for samples with unequal variance.

**Optical coherence tomography (OCT)**

Mice were imaged using a Spectralis OCT as previously described (45). Rats were imaged using the Bioptigen Spectral-domain ophthalmic imaging system (SDOIS), as previously described (39). Briefly, image acquisition was obtained by using the rectangular scanning protocol consisting of a 2 mm by 2 mm perimeter with 750 A-scans (lines) and 5 B-scans (frames) with a 60 Frames/B-scan (for rat retina) or 1.4mm by 1.4mm perimeter with 750 A-scans (lines) and 10 B-scans (frames) with a 20 frames/B-scan (for mouse retina). The Bioptigen InVivoVue Diver 2.0 was used to enable manual segmentation of the retinal layers and the outer nuclear layer thickness was measured after exporting results from Diver to Excel. Statistical analysis was performed using 2 tailed Student's $t$ test for samples with unequal variance, except for the spider plots, which were analysed by 2-way ANOVA with Sidak correction.

## Western blotting and Immunoprecipitation

Retinae were extracted and lysed with RIPA buffer containing 2% (v/v) mammalian protease inhibitor cocktail. Retina lysates were sonicated for $2 \times 15$ s centrifuged for 15 min at $12,000 \times$ g at 4ºC, and diluted in sodium dodecyl sulfate (SDS) sample loading solution. Samples were resolved by SDS-polyacrylamide gel electrophoresis (SDS-PAGE) and western blotting. Immunodetection of rhodopsin was carried out with mouse anti-Rho-1D4 (1:1000; gift from Professor Robert Molday (Department of Biochemistry and Molecular Biology, University of British Columbia, Canada). Blots were probed with anti-mouse (1:50000; 32430, ThermoFisher Scientific) secondary antibodies. Proteins were detected with the ECL Plus reagent (GE Healthcare). For immunoprecipitation, Protein G magnetic Dynabeads (Invitrogen, UK) were incubated with the retinae lysates and with $1 - 4$ μg of specific antibody or $1 - 4$ μg of non-specific IgG overnight at 4C in an end-over-end rotator. Following incubation, the bead–antibody– protein complexes were washed four times with RIPA buffer. Samples were eluted from the beads with 30 μl of 2× SDS buffer, vortexed for 5 s and spun for 1 min at 12 000×g. Supernatant was collected via the Magnarak to minimize magnetic bead contamination. Samples were subjected to SDS – PAGE and western blotting.

## Immunohistochemistry

For fluorescence studies, eyes were collected at specified time points and fixed overnight in 4% paraformaldehyde at 4°C. Post-fixation eyes were cryoprotected by incubation in 30% sucrose in PBS. Eyes were then frozen and cyrosectioned as previously described (45). Cryosectioned eyes were stained with mouse anti-Rho-1D4 (1:1500), mouse anti-HA (1:100, Sigma Aldrich) primary antibodies in blocking

16

solution (3% BSA, 10% normal goat serum) and visualised with Alexa Fluor 488 (1:1000; A11001/A11005, Life Technologies Ltd) and 594 (1:1000; A11007, Life Technologies Ltd) conjugated IgGs. 4',6-diamidino-2-phenylindole dihydrochloride (DAPI) (Sigma Aldrich) staining was used to visualise the nuclei.

**Fluorescence imaging and analysis**

Retina images were obtained using a Carl Zeiss LSM700 laser-scanning confocal microscope. Images were exported with Zen 2009 software were then prepared using Adobe Photoshop and Illustrator CS4. All measurements were performed in ImageJ (http://rsbweb.nih.gov/ij/). Statistical analysis was performed using 2 tailed Student's *t* test for samples with unequal variance.

**Conflict of Interest Statement.**

The authors declare no conflict of interest.

**References**

1      Ferrari, S., Di Iorio, E., Barbaro, V., Ponzin, D., Sorrentino, F.S. and Parmeggiani, F. (2011) Retinitis pigmentosa: genes and disease mechanisms. *Curr. Genomics*, **12**, 238-249.

2      Berson, E.L. (1993) Retinitis pigmentosa. The Friedenwald Lecture. *Invest. Ophthalmol. Vis. Sci.*, **34**, 1659-1676.

3      Hartong, D.T., Berson, E.L. and Dryja, T.P. (2006) Retinitis pigmentosa. *The Lancet*, **368**, 1795-1809.

4      Athanasiou, D., Aguila, M., Bellingham, J., Li, W., McCulley, C., Reeves, P.J. and Cheetham, M.E. (2018) The molecular and cellular basis of rhodopsin retinitis

pigmentosa reveals potential strategies for therapy. *Progress in Retinal and Eye Research*, **62**, 1-23.

5       Dryja, T.P., McGee, T.L., Hahn, L.B., Cowley, G.S., Olsson, J.E., Reichel, E., Sandberg, M.A. and Berson, E.L. (1990) Mutations within the rhodopsin gene in patients with autosomal dominant retinitis pigmentosa. *N. Engl. J. Med.*, **323**, 1302-1307.

6       Mendes, H.F., van der Spuy, J., Chapple, J.P. and Cheetham, M.E. (2005) Mechanisms of cell death in rhodopsin retinitis pigmentosa: implications for therapy. *Trends in molecular medicine*, **11**, 177-185.

7       Chen, Y., Jastrzebska, B., Cao, P., Zhang, J., Wang, B., Sun, W., Yuan, Y., Feng, Z. and Palczewski, K. (2014) Inherent instability of the retinitis pigmentosa P23H mutant opsin. *J. Biol. Chem.*, **289**, 9288-9303.

8       Hwa, J., Reeves, P.J., Klein-Seetharaman, J., Davidson, F. and Khorana, H.G. (1999) Structure and function in rhodopsin: further elucidation of the role of the intradiscal cysteines, Cys-110, -185, and -187, in rhodopsin folding and function. *Proceedings of the National Academy of Sciences of the United States of America*, **96**, 1932-1935.

9       McKibbin, C., Toye, A.M., Reeves, P.J., Khorana, H.G., Edwards, P.C., Villa, C. and Booth, P.J. (2007) Opsin stability and folding: the role of Cys185 and abnormal disulfide bond formation in the intradiscal domain. *Journal of Molecular Biology*, **374**, 1309-1318.

10      Klaips, C.L., Jayaraj, G.G. and Hartl, F.U. (2018) Pathways of cellular proteostasis in aging and disease. *J. Cell Biol.*, **217**, 51-63.

11      Chen, B., Retzlaff, M., Roos, T. and Frydman, J. (2011) Cellular strategies of protein quality control. *Cold Spring Harbor perspectives in biology*, **3**, a004374.

12    Walter, P. and Ron, D. (2011) The Unfolded Protein Response: From Stress Pathway to Homeostatic Regulation. *Science*, **334**, 1081.

13    Athanasiou, D., Kosmaoglou, M., Kanuga, N., Novoselov, S.S., Paton, A.W., Paton, J.C., Chapple, J.P. and Cheetham, M.E. (2012) BiP prevents rod opsin aggregation. *Mol. Biol. Cell*, **23**, 3522-3531.

14    Gorbatyuk, M.S., Knox, T., LaVail, M.M., Gorbatyuk, O.S., Noorwez, S.M., Hauswirth, W.W., Lin, J.H., Muzyczka, N. and Lewin, A.S. (2010) Restoration of visual function in P23H rhodopsin transgenic rats by gene delivery of BiP/Grp78. *Proceedings of the National Academy of Sciences of the United States of America*, **107**, 5961-5966.

15    Pobre, K.F.R., Poet, G.J. and Hendershot, L.M. (2019) The endoplasmic reticulum (ER) chaperone BiP is a master regulator of ER functions: Getting by with a little help from ERdj friends. *J. Biol. Chem.*, **294**, 2098-2108.

16    Cunnea, P.M., Miranda-Vizuete, A., Bertoli, G., Simmen, T., Damdimopoulos, A.E., Hermann, S., Leinonen, S., Huikko, M.P., Gustafsson, J.A., Sitia, R. *et al.* (2003) ERdj5, an endoplasmic reticulum (ER)-resident protein containing DnaJ and thioredoxin domains, is expressed in secretory cells or following ER stress. *J. Biol. Chem.*, **278**, 1059-1066.

17    Hosoda, A., Kimata, Y., Tsuru, A. and Kohno, K. (2003) JPDI, a novel endoplasmic reticulum-resident protein containing both a BiP-interacting J-domain and thioredoxin-like motifs. *J. Biol. Chem.*, **278**, 2669-2676.

18    Ushioda, R., Hoseki, J., Araki, K., Jansen, G., Thomas, D.Y. and Nagata, K. (2008) ERdj5 is required as a disulfide reductase for degradation of misfolded proteins in the ER. *Science*, **321**, 569-572.

19

19      Athanasiou, D., Bevilacqua, D., Aguila, M., McCulley, C., Kanuga, N., Iwawaki, T., Chapple, J.P. and Cheetham, M.E. (2014) The co-chaperone and reductase ERdj5 facilitates rod opsin biogenesis and quality control. *Hum. Mol. Genet.*, **23**, 6594-6606.

20      Molinari, M., Calanca, V., Galli, C., Lucca, P. and Paganetti, P. (2003) Role of EDEM in the release of misfolded glycoproteins from the calnexin cycle. *Science*, **299**, 1397-1400.

21      Oda, Y., Hosokawa, N., Wada, I. and Nagata, K. (2003) EDEM as an acceptor of terminally misfolded glycoproteins released from calnexin. *Science*, **299**, 1394-1397.

22      Kosmaoglou, M., Kanuga, N., Aguila, M., Garriga, P. and Cheetham, M.E. (2009) A dual role for EDEM1 in the processing of rod opsin. *Journal of Cell Science*, **122**, 4465-4472.

23      Insinna, C., Daniele, L.L., Davis, J.A., Larsen, D.D., Kuemmel, C., Wang, J., Nikonov, S.S., Knox, B.E. and Pugh, E.N. (2012) An S-Opsin Knock-In Mouse (F81Y) Reveals a Role for the Native Ligand 11-cis-Retinal in Cone Opsin Biosynthesis. *The Journal of Neuroscience*, **32**, 8094.

24      Braakman, I. and Otsu, M. (2008) Biochemistry. Cargo load reduction. *Science*, **321**, 499-500.

25      Hosoda, A., Tokuda, M., Akai, R., Kohno, K. and Iwawaki, T. (2009) Positive contribution of ERdj5/JPDI to endoplasmic reticulum protein quality control in the salivary gland. *Biochem. J.*, **425**, 117-125.

26      Hagiwara, M., Maegawa, K., Suzuki, M., Ushioda, R., Araki, K., Matsumoto, Y., Hoseki, J., Nagata, K. and Inaba, K. (2011) Structural basis of an ERAD pathway

mediated by the ER-resident protein disulfide reductase ERdj5. *Mol. Cell*, **41**, 432-444.

27      Sakami, S., Maeda, T., Bereta, G., Okano, K., Golczak, M., Sumaroka, A., Roman, A.J., Cideciyan, A.V., Jacobson, S.G. and Palczewski, K. (2011) Probing mechanisms of photoreceptor degeneration in a new mouse model of the common form of autosomal dominant retinitis pigmentosa due to P23H opsin mutations. *J. Biol. Chem.*, **286**, 10551-10567.

28      Behnke, J., Mann, M.J., Scruggs, F.L., Feige, M.J. and Hendershot, L.M. (2016) Members of the Hsp70 Family Recognize Distinct Types of Sequences to Execute ER Quality Control. *Mol. Cell*, **63**, 739-752.

29      Apostolou, E., Moustardas, P., Iwawaki, T., Tzioufas, A.G. and Spyrou, G. (2019) Ablation of the Chaperone Protein ERdj5 Results in a Sjogren's Syndrome-Like Phenotype in Mice, Consistent With an Upregulated Unfolded Protein Response in Human Patients. *Front. Immunol.*, **10**, 506.

30      Mao, H., James, T., Jr., Schwein, A., Shabashvili, A.E., Hauswirth, W.W., Gorbatyuk, M.S. and Lewin, A.S. (2011) AAV delivery of wild-type rhodopsin preserves retinal function in a mouse model of autosomal dominant retinitis pigmentosa. *Hum. Gene Ther.*, **22**, 567-575.

31      Lewin, A.S., Drenser, K.A., Hauswirth, W.W., Nishikawa, S., Yasumura, D., Flannery, J.G. and LaVail, M.M. (1998) Ribozyme rescue of photoreceptor cells in a transgenic rat model of autosomal dominant retinitis pigmentosa. *Nat. Med.*, **4**, 967-971.

32      Murray, S.F., Jazayeri, A., Matthes, M.T., Yasumura, D., Yang, H., Peralta, R., Watt, A., Freier, S., Hung, G., Adamson, P.S. *et al.* (2015) Allele-Specific

Inhibition of Rhodopsin With an Antisense Oligonucleotide Slows Photoreceptor Cell Degeneration. *Invest. Ophthalmol. Vis. Sci.*, **56**, 6362-6375.

33      Millington-Ward, S., Chadderton, N., O'Reilly, M., Palfi, A., Goldmann, T., Kilty, C., Humphries, M., Wolfrum, U., Bennett, J., Humphries, P. *et al.* (2011) Suppression and replacement gene therapy for autosomal dominant disease in a murine model of dominant retinitis pigmentosa. *Mol. Ther.*, **19**, 642-649.

34      Cideciyan, A.V., Sudharsan, R., Dufour, V.L., Massengill, M.T., Iwabe, S., Swider, M., Lisi, B., Sumaroka, A., Marinho, L.F., Appelbaum, T. *et al.* (2018) Mutation-independent rhodopsin gene therapy by knockdown and replacement with a single AAV vector. *Proceedings of the National Academy of Sciences of the United States of America*, **115**, E8547-E8556.

35      Giannelli, S.G., Luoni, M., Castoldi, V., Massimino, L., Cabassi, T., Angeloni, D., Demontis, G.C., Leocani, L., Andreazzoli, M. and Broccoli, V. (2018) Cas9/sgRNA selective targeting of the P23H Rhodopsin mutant allele for treating retinitis pigmentosa by intravitreal AAV9.PHP.B-based delivery. *Hum. Mol. Genet.*, **27**, 761-779.

36      Li, P., Kleinstiver, B.P., Leon, M.Y., Prew, M.S., Navarro-Gomez, D., Greenwald, S.H., Pierce, E.A., Joung, J.K. and Liu, Q. (2018) Allele-Specific CRISPR-Cas9 Genome Editing of the Single-Base P23H Mutation for Rhodopsin-Associated Dominant Retinitis Pigmentosa. *CRISPR J.*, **1**, 55-64.

37      Chiang, W.C., Kroeger, H., Sakami, S., Messah, C., Yasumura, D., Matthes, M.T., Coppinger, J.A., Palczewski, K., LaVail, M.M. and Lin, J.H. (2015) Robust Endoplasmic Reticulum-Associated Degradation of Rhodopsin Precedes Retinal Degeneration. *Mol. Neurobiol.*, **52**, 679-695.

38      Sakami, S., Kolesnikov, A.V., Kefalov, V.J. and Palczewski, K. (2014) P23H opsin knock-in mice reveal a novel step in retinal rod disc morphogenesis. *Hum. Mol. Genet.*, **23**, 1723-1741.

39      Athanasiou, D., Aguila, M., Bellingham, J., Kanuga, N., Adamson, P. and Cheetham, M.E. (2017) The role of the ER stress-response protein PERK in rhodopsin retinitis pigmentosa. *Hum. Mol. Genet.*, **26**, 4896-4905.

40      Humphries, M.M., Rancourt, D., Farrar, G.J., Kenna, P., Hazel, M., Bush, R.A., Sieving, P.A., Sheils, D.M., McNally, N., Creighton, P. *et al.* (1997) Retinopathy induced in mice by targeted disruption of the rhodopsin gene. *Nat. Genet.*, **15**, 216-219.

41      Hulleman, J.D., Genereux, J.C. and Nguyen, A. (2016) Mapping wild-type and R345W fibulin-3 intracellular interactomes. *Exp. Eye Res.*, **153**, 165-169.

42      Lobanova, E.S., Finkelstein, S., Li, J., Travis, A.M., Hao, Y., Klingeborn, M., Skiba, N.P., Deshaies, R.J. and Arshavsky, V.Y. (2018) Increased proteasomal activity supports photoreceptor survival in inherited retinal degeneration. *Nat. Commun.*, **9**, 1738.

43      Dong, M., Bridges, J.P., Apsley, K., Xu, Y. and Weaver, T.E. (2008) ERdj4 and ERdj5 are required for endoplasmic reticulum-associated protein degradation of misfolded surfactant protein C. *Mol. Biol. Cell*, **19**, 2620-2630.

44      Nishiguchi, K.M., Carvalho, L.S., Rizzi, M., Powell, K., Holthaus, S.-M.k., Azam, S.A., Duran, Y., Ribeiro, J., Luhmann, U.F.O., Bainbridge, J.W.B. *et al.* (2015) Gene therapy restores vision in rd1 mice after removal of a confounding mutation in Gpr179. *Nat. Commun.*, **6**, 6006.

45      Aguila, M., Bevilacqua, D., McCulley, C., Schwarz, N., Athanasiou, D., Kanuga, N., Novoselov, S.S., Lange, C.A., Ali, R.R., Bainbridge, J.W. *et al.* (2014)

Hsp90 inhibition protects against inherited retinal degeneration. *Hum. Mol. Genet.*,

**23**, 2164-2175.

**Legends to Figures**
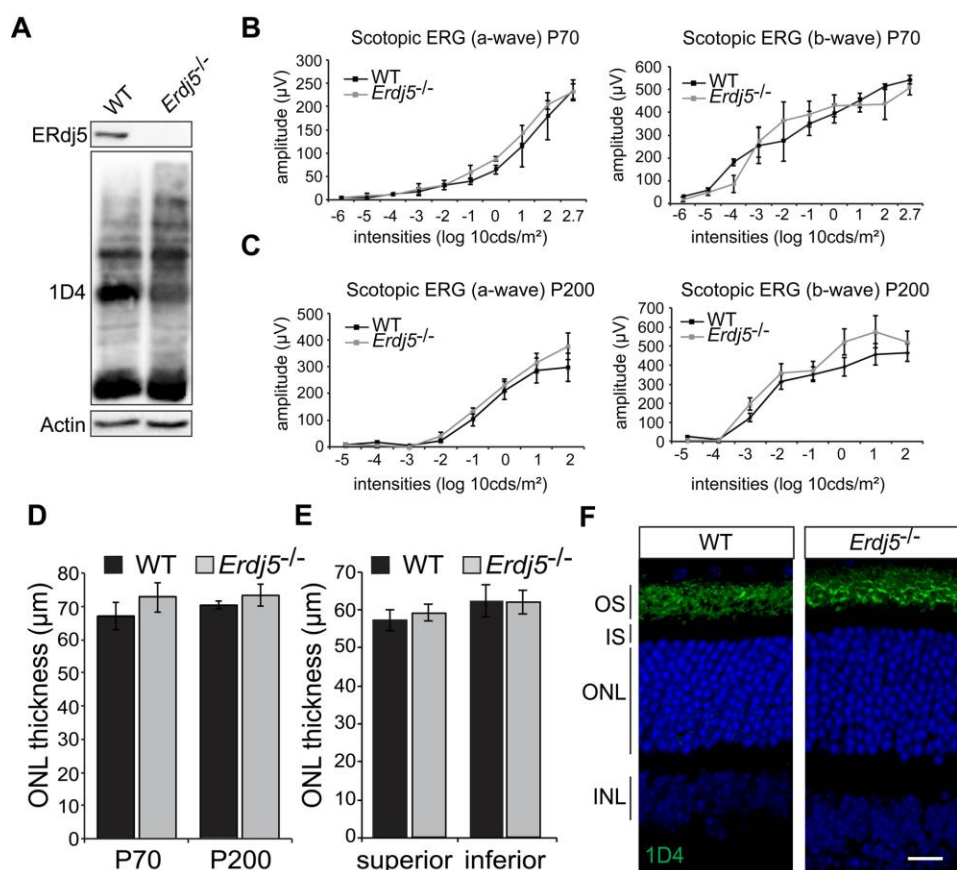


**Figure 1**. *Erdj5 knockout mice do not show retinal degeneration*. (**A**) Western blot of WT and *Erdj5*^{-/-} retina lysate probed with ERdj5 and 1D4 anti-rhodopsin antibody. Actin immunoreactivity was used as a loading control. Scotopic ERG responses, a and b wave of WT and *Erdj5*^{-/-} mice at (**B**) P70 (n=4) and (**C**) P200 (n=4). (**D-E**) ONL thickness measurements assessed by OCT of the total retina (**D**), and superior and inferior hemispheres (**E**). (**F**) Representative images of WT and *Erdj5*^{-/-} (P200) retina sections with rhodopsin stained in green and nuclei in blue with DAPI. Scale bars = 10 μm.
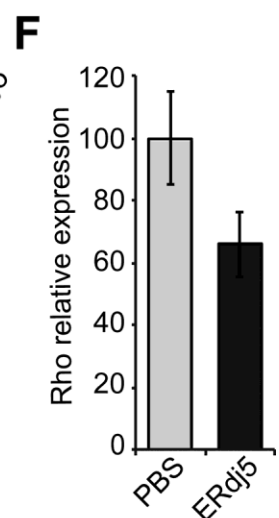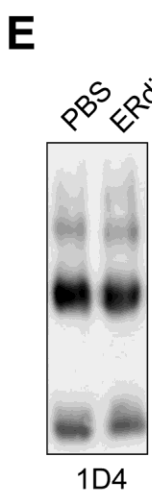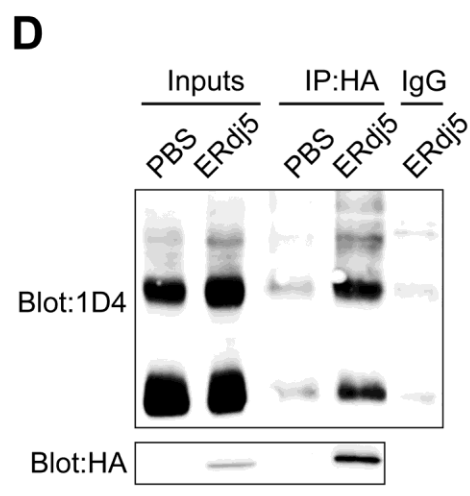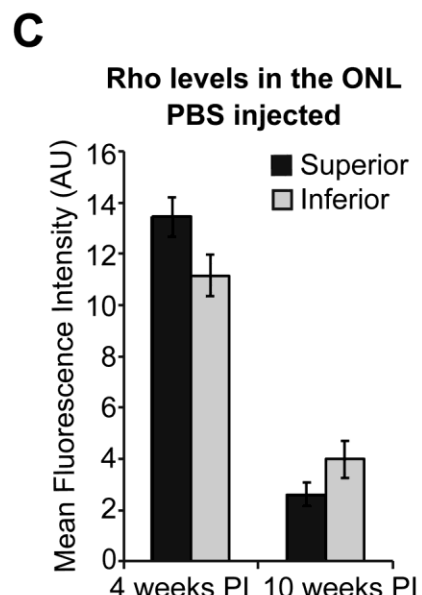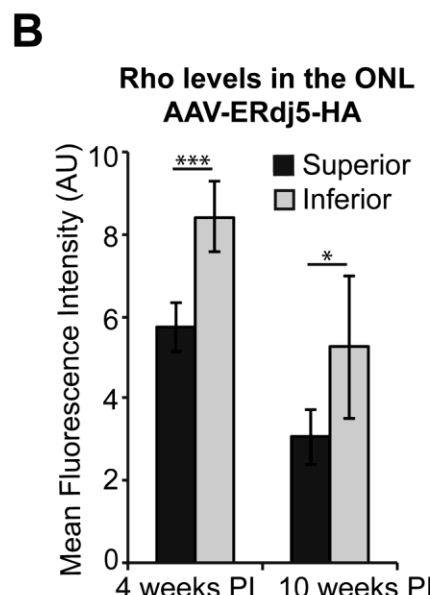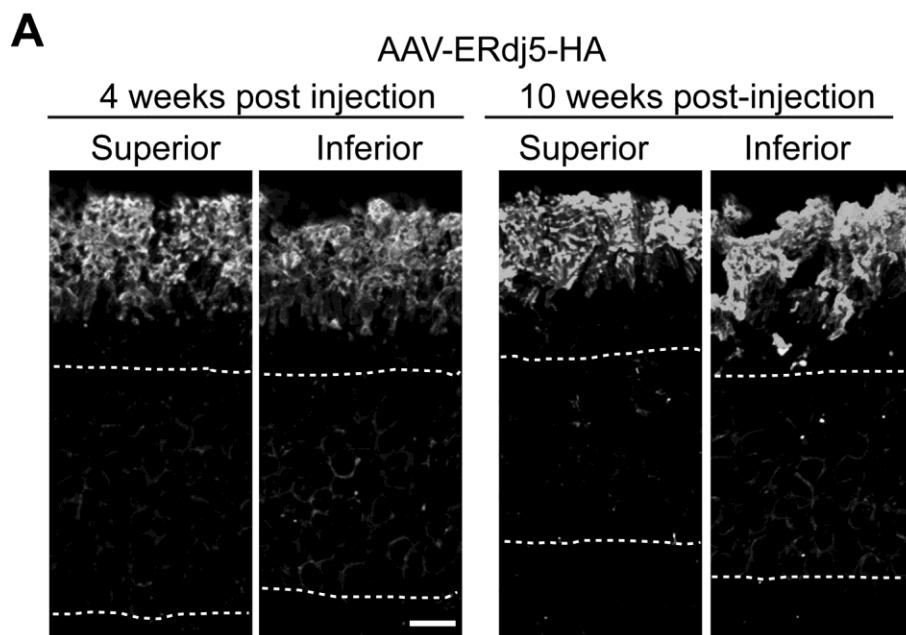
25
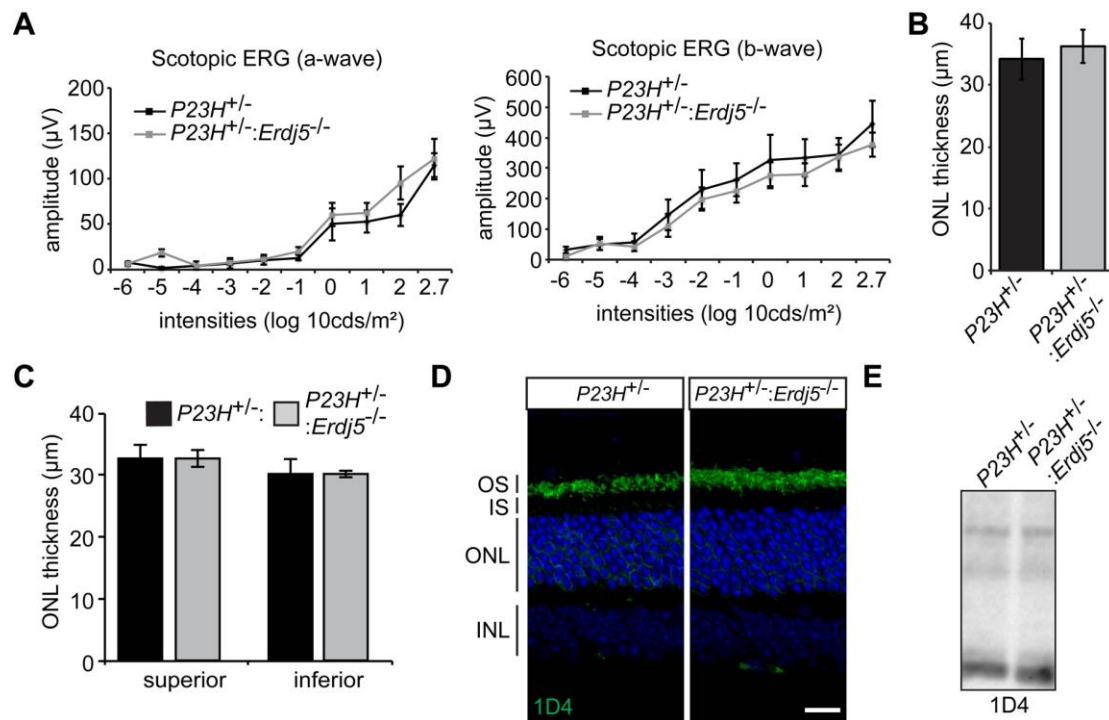
**Figure 2**. *Erdj5 ablation does not affect retinal degeneration in P23H rhodopsin mice*. (**A**) Scotopic ERG responses of the *P23H$^{+/-}$:Erdj5$^{-/-}$* animals compared to *P23H$^{+/-}$* (n=4). (**B**) Western blot of the *P23H$^{+/-}$* and *P23H$^{+/-}$:Erdj5$^{-/-}$* retinal lysates probed for rhodopsin with the 1D4 antibody. (**C-D**) ONL thickness measurements assessed by OCT for the total retina (**C**) and superior and inferior hemispheres (**D**). (**E**) Representative confocal images of *P23H$^{+/-}$* and *P23H$^{+/-}$:Erdj5$^{-/-}$* retina showing no difference in retinal structure or rhodopsin localization between genotypes. Scale bars = 10 μm

26
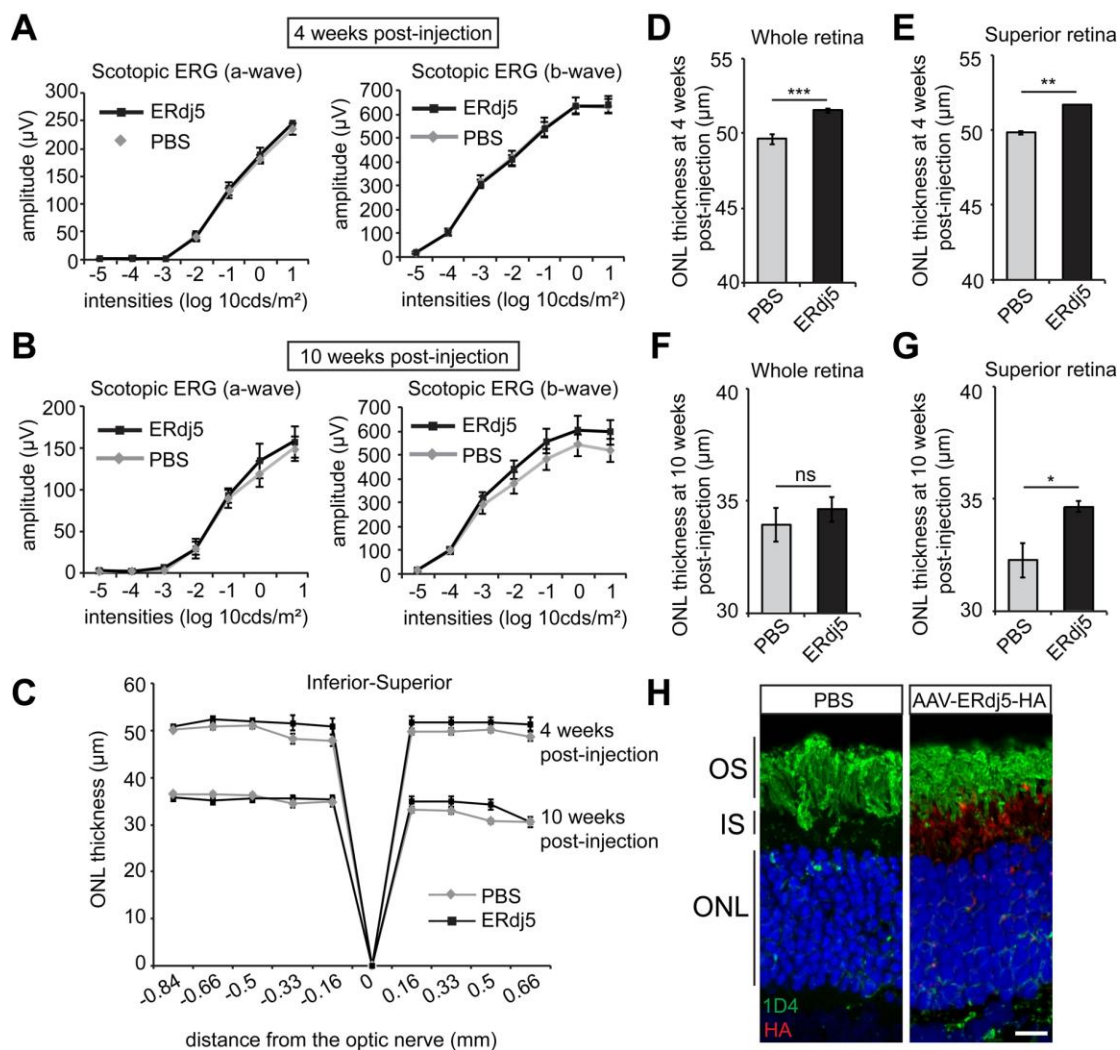
**Figure 3**. *ERdj5 gene augmentation enhances photoreceptor survival in P23H-3 rats.* Scotopic ERG responses of P23H-3 rats subretinally injected with PBS or AAV-ERdj5-HA assessed 4 weeks post-injection (**A**) and 10 weeks post-injection (**B**) (n=8). (**C**) Spider plot showing P23H-3 ONL thickness at 4 and 10 weeks after PBS or AAV-ERdj5-HA injection assessed by OCT (n=8). Mean ONL thickness across the whole retina (**D**, **F**) and the superior retina (subretinal injection site) (**E**, **G**) at 4 weeks (**D**, **E**) and 10 weeks (**F**, **G**) post-injection (n=8). (**H**) Representative image of P23H-3 rat retina 4 weeks post-injection with PBS or AAV-ERdj5-HA at 6 weeks of age and stained with 1D4 antibody (green) and HA antibody (red). Scale bar = 10μm. ns not significant * p<0.05; ** p<0.01; *** p<0.001

27

**A** AAV-ERdj5-HA

4 weeks post injection — Superior, Inferior

10 weeks post-injection — Superior, Inferior

**B** Rho levels in the ONL AAV-ERdj5-HA

Mean Fluorescence Intensity (AU) vs 4 weeks PI, 10 weeks PI

■ Superior ■ Inferior

*** (4 weeks PI), * (10 weeks PI)

**C** Rho levels in the ONL PBS injected

Mean Fluorescence Intensity (AU) vs 4 weeks PI, 10 weeks PI

■ Superior ■ Inferior

**D** Inputs | IP:HA | IgG — PBS, ERdj5, PBS, ERdj5, ERdj5

Blot:1D4

Blot:HA

**E** PBS, ERdj5 — 1D4

**F** Rho relative expression — PBS, ERdj5

**Figure 4**. *ERdj5 overexpression promotes rhodopsin degradation*. (**A**) Representative images of the superior and inferior retina of P23H-3 rats injected with AAV-ERdj5-HA and stained for rhodopsin at 4 and 10 weeks post-injection (PI), 6 and 12 weeks of age respectively. ONL marked with a dotted line. (**B**-**C**) Quantification of rhodopsin immunofluorescence intensity in the ONL showing increased levels of rhodopsin in the inferior retina in AAV-treated eyes (**B**), but not in control PBS-injected eyes (**C**) (n=3). (**D**) Co-immunoprecipitation of rhodopsin with ERdj5, 4 weeks post-injection retinal lysates of PBS or AAV-ERdj5-HA injected eyes were incubated overnight with HA antibody (IP:HA) or control IgG (IgG) and immunopurified material was blotted with 1D4 antibody against rhodopsin. (**E**) Western blot of P23H-3 retinae injected with PBS or AAV-ERdj5-HA and probed with the 1D4 antibody. (**F**) Densitometric analysis was used to calculate the levels of rhodopsin in the AAV-ERdj5-HA injected retinae relative to the PBS injected (n=4). * $p < 0.05$; *** $p < 0.001$. Scale bar = 10μm.

## Abbreviations

| | |
|---|---|
| AAV | adeno associated viral |
| adRP | autosomal dominant retinitis pigmentosa (adRP |
| ERG | Electroretinogram |
| ERAD | ER-associated degradation (ERAD) |
| EDEM1 | ER degradation-enhancing alpha-mannosidase-like 1 |
| INL | inner nuclear layer |
| IS | inner segment |
| ITR | Inverted Terminal Repeat |
| KI | knock-in |
| OCT | optical coherence tomography |
| ONL | outer nuclear layer |
| OS | outer segment |
| RP | Retinitis Pigmentosa |
| SDS | sodium dodecyl sulfate |
| SDS-PAGE | SDS-polyacrylamide gel electrophoresis |
| SD | Sprague Dawley |
| TRX | thioredoxin-like |
| UPR | unfolded protein response |
| WT | wild-type |